Laser-assisted biomineralization on human dentin for tooth surface functionalization

Ayako Oyane[*,1], Noriyuki Saito[2], Ikuko Sakamaki[1], Kenji Koga[1], Maki Nakamura[1], A. Joseph Nathanael[1], Noriko Yoshizawa[2], Kanako Shitomi[3], Kayoko Mayumi[3], Hirofumi Miyaji[3]

[1]*Nanomaterials Research Institute, National Institute of Advanced Industrial Science and Technology (AIST), Central 5, 1-1-1 Higashi, Tsukuba, Ibaraki 305-8565, Japan*

[2]*Tsukuba Innovation Arena (TIA), National Institute of Advanced Industrial Science and Technology (AIST), Central 5, 1-1-1 Higashi, Tsukuba, Ibaraki 305-8565, Japan*

[3]*Department of Periodontology and Endodontology, Faculty of Dental Medicine, Hokkaido University, N13W7, Kita-ku, Sapporo, Hokkaido 060-8586, Japan*

Declarations of interest: none

* Corresponding author: **Ayako Oyane, Ph.D.,**

Nanomaterials Research Institute, National Institute of Advanced Industrial Science and Technology (AIST), Central 5, 1-1-1 Higashi, Tsukuba, Ibaraki 305-8565, Japan

Tel:+81-29-861-4693, Fax:+81-29-861-3005

E-mail: a-oyane@aist.go.jp

ABSTRACT

A technique for tooth surface modification with biocompatible calcium phosphate (CaP) has huge potential in dental applications. Recently, we achieved a facile and area-specific CaP coating on artificial materials by a laser-assisted biomimetic process (LAB process), which consists of pulsed laser irradiation in a supersaturated CaP solution. In this study, we induced the rapid biomineralization on the surface of human dentin by using the LAB process. A human dentin substrate was immersed in a supersaturated CaP solution, then its surface was irradiated with weak pulsed laser light for 30 min (LAB process). Ultrastructural analyses revealed that the pristine substrate had a demineralized collagenous layer on its surface due to the previous EDTA surface cleaning. After the LAB process, this collagenous layer disappeared and was replaced with a submicron-thick hydroxyapatite layer. We believe that the laser irradiation induced pseudo-biomineralization through the laser ablation of the collagenous layer, followed by CaP nucleation and growth at the dentin–liquid interface. The mineralized layer on the dentin substrate consisted of needle-like hydroxyapatite nanocrystals, whose *c*-axes were weakly oriented along the direction perpendicular to the substrate surface. This LAB process would offer a new tool enabling tooth surface modification and functionalization through the *in situ* pseudo-biomimeralization.

Keywords: Hydroxyapatite, Calcium phosphate (CaP), Dentin, Laser, Biomimetic process, Coating

Abbreviations

AIST, Advanced Industrial Science and Technology; CaP, Calcium Phosphate; LAB, Laser-assisted biomimetic; OCP, Octacalcium phosphate; EDTA, ethylenediaminetetraacetic acid; SEM, Scanning electron microscope; EDX, Energy-dispersive X-ray; FT-IR, Fourier transform infrared; ATR, Attenuated total reflection; XRD, X-ray diffraction; FIB, Focused ion beam; TEM, Transmission electron microscope; HAADF, High-angle annular dark field; STEM, Scanning transmission electron microscopy; HRTEM; high-resolution TEM; SAED, Selected area electron diffraction

1. Introduction

Calcium phosphate (CaP) is the main inorganic component (biomineral) of mineralized human hard tissues, such as bones and teeth. Certain types of CaP compounds, such as hydroxyapatite and β-tricalcium phosphate, exhibit good biocompatibility and osteoconductibity, and have thus been used in a wide variety of biomaterials [1-4]. The physiological CaP formation (biomineralization) in body fluids can be mimicked *in vitro* by using acellular supersaturated CaP solutions (typically, a simulated body fluid) [5]. Pseudo-biomineralization reactions in supersaturated CaP solutions have been used as low-temperature CaP coating processes on artificial materials (a biomimetic process) [6-9]. Biomimetic processes offer the advantages of using a bio-friendly reaction media and mild reaction conditions, compared to other prevalent CaP coating processes (plasma and thermal spraying, pulsed laser deposition, etc. [10,11]). In biomimetic processes, the nano- and micro-structures, composition, and even the biological functions of the resulting CaP coatings can be controlled by fine-tuning the reaction conditions [7,8,12,13].

In spite of their advantages, biomimetic processes are not widely used due to their practical disadvantages; *i.e.*, relatively long processing times (generally one day or more) and complex procedures involving a previous surface-modification step. Recently, we developed a laser-assisted biomimetic (LAB) process that enabled rapid, one-step CaP coating on various materials with laser absorption [14,15]. In this process, a substrate surface is irradiated with low-energy pulsed laser light in a supersaturated CaP solution (CP solution [16]). Within 30 min, the irradiated area of the surface is coated with hydroxyapatite or its precursor phase, octacalcium phosphate (OCP). Although there are several reports on biomimetic processes assisted by laser irradiation [17,18], they require multiple steps to produce CaP coatings on materials, *i.e.*, a laser-assisted

surface modification step followed by a CaP growth/aging step. Until now, the LAB process for one-step CaP coating has been applied to polymeric [14,19,20], ceramic [21,22], metallic [23,24], and ceramic–polymer composite [25] materials.

We believed that pseudo-biomineralization can be induced on a human tooth surface by utilizing the LAB process, that is, pulsed laser irradiation in the CP solution. If laser-assisted rapid biomineralization is achieved at a specific region of the tooth surfaces, then this process would be a new technique for tooth surface modification and functionalization. Such a technique has immense potential in dental applications. For example, it may reduce the risk of recurrence of periodontal diseases: highly prevalent ailments affecting up to 90% of elderly people [26]. In periodontal flap surgery, a gingival flap is elevated to expose the diseased tooth root and then dental plaque and calculus are mechanically removed from root surface. However, the surface biocompatibility of the post-operative tooth is inferior to that of the healthy natural tooth, and has difficulties to reconstruct the periodontal attachment [27-29]. The lack of periodontal attachment could allow bacterial invasion, colonization, and biofilm development, and hence, often leads to recurrent periodontal diseases. If a post-operative damaged tooth surface is modified with biocompatible CaPs by laser-assisted biomineralization, the resulting surface could possess improved resistance against recurrent periodontal diseases.

In the present study, we induced the rapid biomineralization on a human dentin substrate by using the LAB process, and demonstrated its potential in tooth surface modification. Figure 1 shows a schematic flow chart of this study. First, tabular dentin substrates were prepared from donated teeth that were extracted in standard dental treatments. The substrates were cleaned with a clinically approved smear removal agent, ethylenediaminetetraacetic acid (EDTA). Then, the LAB process was applied to the dentin substrate using the CP solution as reaction medium. The

surfaces and cross-sections of the unprocessed and LAB-processed substrates were analyzed to evaluate the effect of the LAB process on biomineralization on the dentin surface.

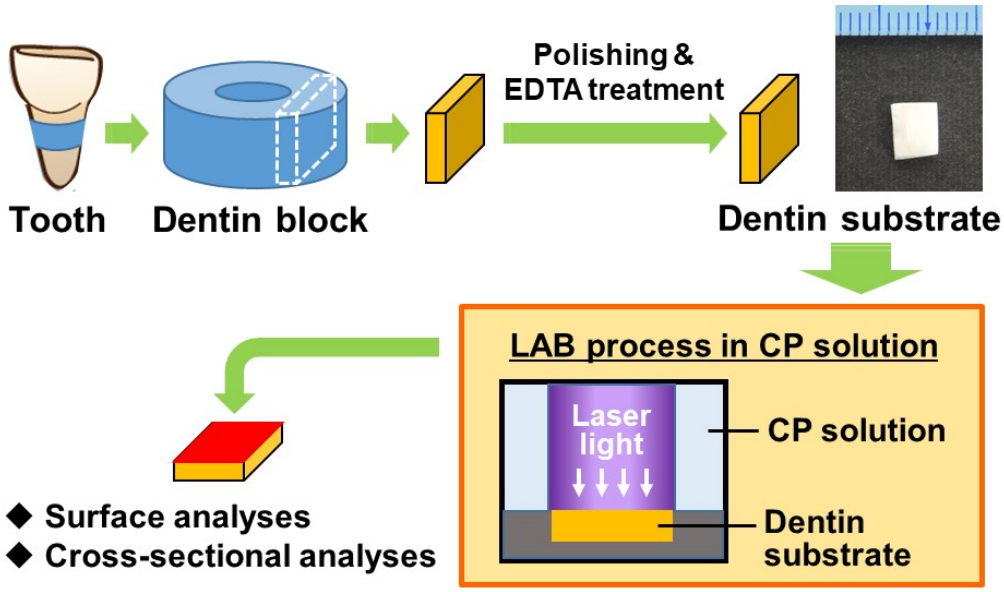

Figure 1. Flow chart of the present research.

2. Materials and methods

2.1. Preparation of dentin substrates

This study was conducted in compliance with the Declaration of Helsinki and was performed according to the conditions approved by the ethical review boards of both the Hokkaido University Hospital for clinical research (approval No. 16-72) and the National Institute of Advanced Industrial Science and Technology (AIST) in Japan. Informed consent was obtained from patients at the dental department of the Hokkaido University Hospital.

Dentin substrates were prepared from vital third molars extracted in standard treatments at the dental department of the Hokkaido University Hospital from 20 to 40 years old patients. The tooth root was shaped with a diamond disk (Horico diamond disk 87xFSI, HORICO DENTAL

Hopf, Ringleb & Co. GmbH & Cie., Germany) to obtain 1-mm thick tabular dentin substrates of 2–4 × 5–6 mm (Figure 1). The surface of the dentin substrates were polished first with #600 and then with #2000 SiC polishing papers (FUJI STAR DCCS, Sankyo-Rikagaku Co., Ltd, Japan), and washed ultrasonically with pure water. The substrates were then treated for 5 min with a 3% EDTA solution (Smear Clean, Nippon Shika Yakuhin Co., Ltd., Japan) under ultrasonication for smear removal and surface cleaning. Finally, the substrates were again washed ultrasonically with pure water for 1 min. All the ultrasonic cleaning steps were carried out at room temperature using an ultrasonic cleaner (VS-100III, AS ONE Corporation, Japan). The thus-prepared dentin samples (referred to as unprocessed substrates) were kept at −20°C before use.

2.2. Preparation of the CP solution

The CP solution was prepared according to a previously described protocol [16,22]. First, reagent grade (Nacalai Tesque, Inc., Japan) NaCl (142 mM final concentration), $K_2HPO_4 \cdot 3H_2O$ (1.50 mM final concentration), 1M HCl (40 mM final concentration), and $CaCl_2$ (3.75 mM final concentration) were dissolved in ultrapure water, one reagent at a time. Then, a buffering agent, tris(hydroxymethyl)aminomethane (50 mM final concentration) and 1M HCl (amount necessary for pH adjustment) were slowly added to the solution to achieve a final pH of 7.40 at 25.0°C. The as-prepared CP solution was tightly sealed in a polystyrene bottle and stored at 4°C before use for a maximum of 4 weeks.

2.3. LAB process for CaP coating

The LAB process for the dentin substrates was performed under the conditions optimized for a sintered hydroxyapatite substrate [22]. The substrate was set on the bottom of a glass bottle

using a poly(tetrafluoroethylene) holder. Soon after adding 5 mL of the CP solution to the bottle (substrate was fully immersed in the solution), the bottle was placed in a constant temperature water bath (25°C). Nanosecond pulsed laser irradiation (λ = 355 nm, 6 W/cm^2, 30 Hz) was applied without focusing to the dentin surface with a Nd:YAG laser (Quanta-Ray LAB-150-30, Spectra-Physics, USA). Temperature of the CP solution was monitored during the LAB process using a digital thermometer (PC-3300, Sato Keiryoki Mfg. Co., Ltd, Japan). After irradiation for 30 min, the substrate was removed from the solution, washed gently with ultrapure water, and dried at room temperature. The CP solution did not induce homogeneous CaP precipitation and was transparent throughout the irradiation process. The LAB-processed substrates were maintained in a desiccator before use.

2.4. Control experiments

As a control experiment to clarify the role of laser irradiation in the LAB process, the dentin substrate was immersed at 25°C for 30 min in the CP solution without laser irradiation. As another control experiment, laser irradiation was performed in the same manner described in Section 2.3, except that ultrapure water was used in place of the CP solution to assess changes of the bare dentin surface (without CaP) in the LAB process.

2.5. Surface analyses

Images of the unprocessed dentin substrates were captured with a digital camera (COOLPIX P330, Nikon Corporation, Japan). The surface morphology and chemical composition of the substrate before and after the process were analyzed using a scanning electron microscope (SEM; model XL30, FEI Company, USA and S-4800, Hitachi High-Technologies Corporation, Japan)

equipped with an energy-dispersive X-ray (EDX) analyzer (EMAX x-act, HORIBA, Ltd., Japan). Before the SEM-EDX analyses, the substrates were sputter-coated with carbon using a carbon coater (VC-100, Vacuum device Co., Ltd., Japan). The chemical bonds of the substrates' surfaces were examined using a Fourier transform infrared (FT-IR) spectrometer (FT/IR-4700, JASCO Corporation, Japan) equipped with an attenuated total reflection (ATR) accessory with a monolithic diamond crystal. The crystalline structure of the substrate surfaces was examined using an X-ray diffraction (XRD) analyzer (M18X, MacScience, Japan) with Cu Kα radiation (λ = 0.154178 nm).

2.6. Cross-sectional analyses

Cross-sectional ultra-thin samples were prepared from the substrates before and after the LAB process *via* a conventional focused ion beam (FIB) technique. For precise comparison, the substrates used were prepared from the same molar because the physicochemical properties of human dentin differ between individuals (*e.g.*, crystallinity, carbonate content, etc. [30]). Before FIB processing with a Ga^+ ion source (FB-2100, Hitachi, Japan), the substrates were coated with a chromium (Cr)-containing oil-based ink to protect the surface. Then, FIB processing was performed for tungsten (W) protection coating (deposited from $W(CO)_6$ gas) and subsequent preparation of the cross-sectional samples. Each sample was then mounted on a molybdenum (Mo) FIB lift-out grid, and thinned to approximately 100 nm.

The prepared cross-sectional ultra-thin samples were analyzed using an analytical transmission electron microscope (TEM; Tecnai Osiris, FEI, USA) operating at 200 kV. The TEM was equipped with an EDX analyzer (Super-X system, FEI, USA) and a high-angle annular dark field (HAADF) scanning transmission electron microscopy (STEM) system with a probe diameter

of less than 1 nm. In the quantitative STEM-EDX analysis, 2–3 different regions on the sample were analyzed to calculate the average and standard deviation.

3. **Results and discussion**

3.1. Surface analyses

During the LAB process, the surface morphology of the dentin substrate was modified at the submicrometer scale, although no significant changes in the surface composition were observed by SEM-EDX (Figure 2). As shown in the lower magnification SEM images (Figure 2a top), both the unprocessed and LAB-processed dentin substrates had several micro-holes running in the same direction on their surfaces. These micro-holes must be the dentinal canaliculi, also called dentinal tubules. According to the magnified SEM images (Figure 2a bottom), the smooth dentin surface roughened after the LAB process. The LAB-processed dentin surface was covered with densely assembled submicrometer particles, as seen in the inset of the lower right image in Figure 2a. The SEM-EDX spectra in Figure 2b show that both substrates had similar surface compositions; the main components were Ca, P, and O.

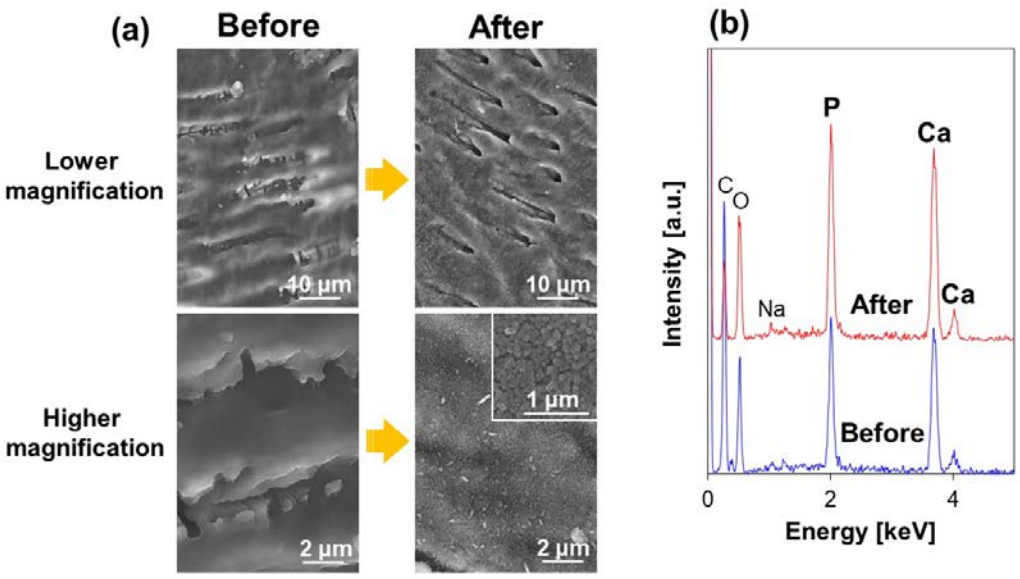

Figure 2. (a) Higher and lower magnifications of SEM images, (b) SEM-EDX spectra of the surfaces of the dentin substrates before and after the LAB process. The C peak in (b) corresponds to the carbon coating and the substrates.

The morphological change found on the surface of the LAB-processed dentin substrate was attributed to the formation of *c*-axis-oriented hydroxyapatite crystals, according to the XRD (Figure 3) results. The XRD patterns presented in Figure 3a clearly indicate that the peaks before and after the LAB process correspond to hydroxyapatite. After the process, the peak intensities remarkably increased, and some new minor peaks appeared at ~23, 42, 44, and 45^0. Particularly, there was an outstanding intensity increase of the 002 peak located at ~26^0. This might be caused by the *c*-axis orientation of the newly formed hydroxyapatite crystals along the direction perpendicular to the dentin surface; this was confirmed by the selected area electron diffraction (SAED) analysis in Section 3.5. Additionally, we evaluated whether an OCP phase was present before and after the LAB process, but no peak was detected at 4.7^0 (main peak position of OCP, JCPDS card #261056) (Figure 3b), suggesting that the amount of OCP was under the detection limit. As shown in the FT-IR spectra (Figure 4), the unprocessed dentin surface had reflection

peaks ascribed to phosphate (PO_4) and carbonate (CO_3) bonds, in addition to amide bond [31,32]. This agrees with the fact that human dentin is mainly composed of type I collagen and carbonate hydroxyapatite. After the LAB process, the intensity of the phosphate peak significantly increased, whereas that of the amide peak decreased.

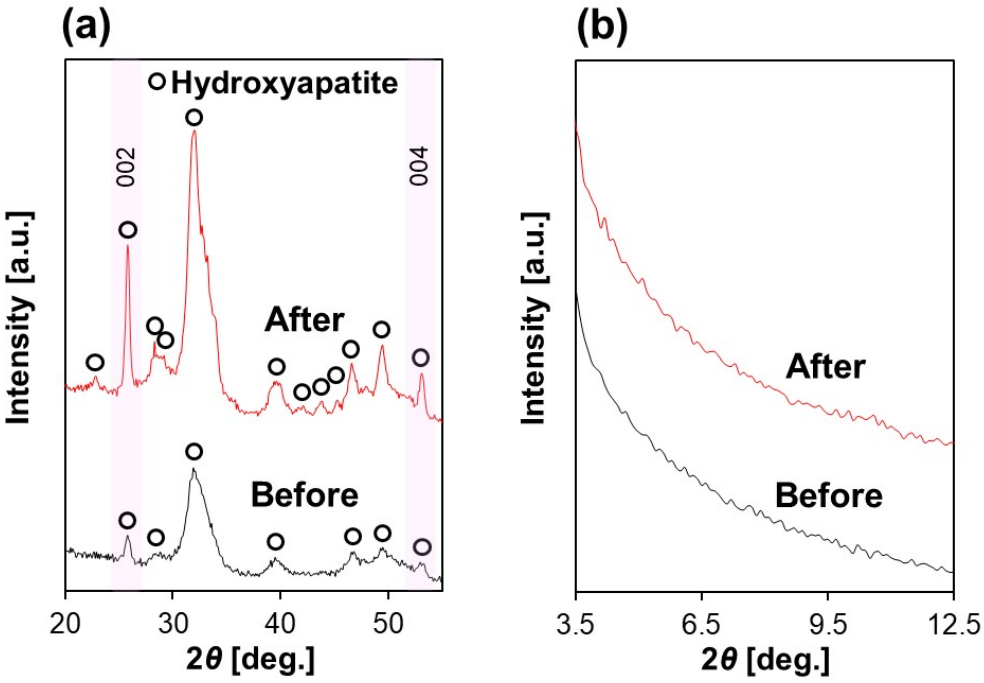

Figure 3 2θ/θ XRD patterns (a: wide range, b: narrow range) of the surfaces of the dentin substrates before and after the LAB process.

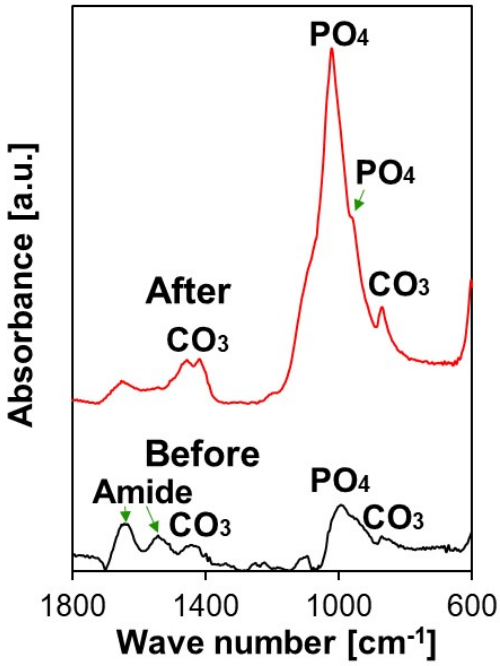

Figure 4. FT-IR spectra of the surfaces of the dentin substrates before and after the LAB process.

3.2. Immersion in the CP solution without laser irradiation

Laser irradiation was critical to induce the hydroxyapatite formation on the dentin surface. This was verified by analyzing the changes in a dentin substrate that was immersed for 30 min in the CP solution without laser irradiation. Compared to the unprocessed substrate (see "Before" in Figures 2a and 4), the resulting substrate showed no significant difference in the surface morphology (Figure 5a) nor in the surface chemical bonds (Figure 5b). Thus, without the laser irradiation, the dentin substrate did not form hydroxyapatite on its surface, even after immersion in the CP solution for 30 min.

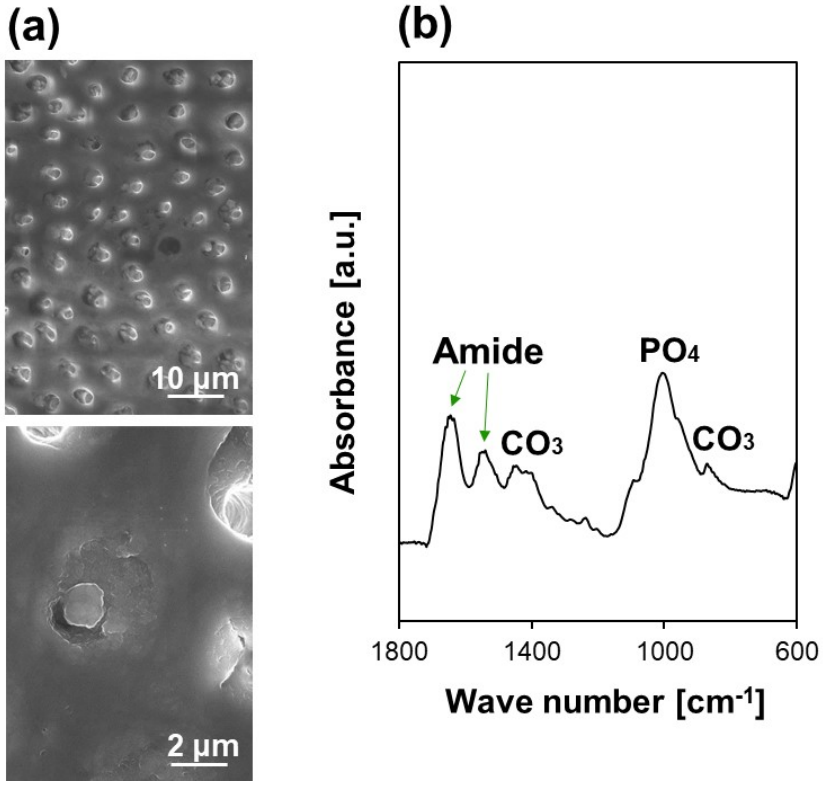

Figure 5 (a) Higher (bottom) and lower (top) magnifications of SEM images and (b) FT-IR spectrum of the surface of the dentin substrate after the comparison test; the substrate was immersed in the CP solution for 30 min without laser irradiation.

3.3. Laser irradiation in ultrapure water

Laser irradiation in ultrapure water induced significant changes in the surface chemical bonds, whereas it did not cause an apparent morphological change on the dentin surface. As shown in Figure 6a, morphology of the laser-irradiated dentin surface was similar to that of the unprocessed surface (see "Before" in Figure 2a). On the other hand, FT-IR spectrum of the laser-irradiated dentin surface (Figure 6b) was largely different from that of the unprocessed surface (see "Before" in Figure 4); the intensity of the phosphate peak significantly increased, whereas that of the amide group decreased after laser irradiation in ultrapure water. The observed change is similar to that

found in the LAB process (Figure 4). Thus, laser irradiation affects surface chemistry of the dentin substrate as detailed in Section 3.5.

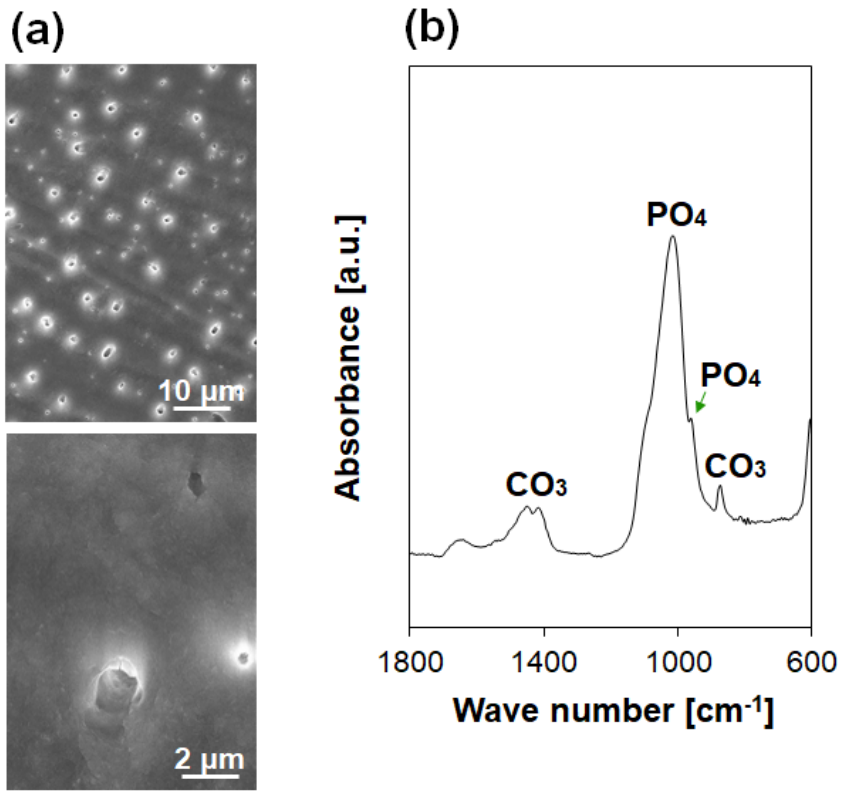

Figure 6 (a) Higher (bottom) and lower (top) magnifications of SEM images and (b) FT-IR spectrum of the surface of the dentin substrate after the comparison test; the substrate was irradiated with pulsed laser light for 30 min in ultrapure water.

3.4. Cross-sectional analyses of the unprocessed dentin substrate

Figure 7a shows the cross-sectional bright-field TEM image of the unprocessed substrate. The uppermost black layer is the W coating formed on the substrate during the FIB processing. Fine needle-like structures, typical of dentinal hydroxyapatite, were observed throughout the depth of the substrate except for the upper surface, where submicron-thick double layers existed (see below the W coating). In the high-resolution TEM (HRTEM) image (Figure 7c), lattice patterns

indexed as the (0 0 2) and (1 0 0) planes of hydroxyapatite were observed. In the SAED pattern (Figure 7b) obtained from the circled area in Figure 7a, arcs of the hydroxyapatite (0 0 2) reflection were observed along with the continuous Debye ring of the (2 1 1), (1 2 1), and (1 1 2) reflections. The result suggests that the needle-like hydroxyapatite nanocrystals in the highlighted area were weakly oriented along the *c*-axis (two-way arrow in Figure 7a). Since the direction of the *c*-axis orientation randomly varied from one section to another, the dentin substrate as a whole had no significant crystalline orientation. Figures 8a and 8b display the cross-sectional STEM-EDX elemental mappings (Ca, P, O, N, C, Cr) and the corresponding HAADF image, respectively, of the unprocessed dentin substrate, and Figure 8c displays STEM-EDX spectra of the boxed areas in Figure 8b. According to the STEM-EDX results, the hydroxyapatite in the unprocessed dentin substrate possessed a Ca/P elemental ratio of 1.64 ± 0.01. Heavy elements, Ga, W, and Mo, detected by STEM-EDX are due to the FIB processing and TEM grids.

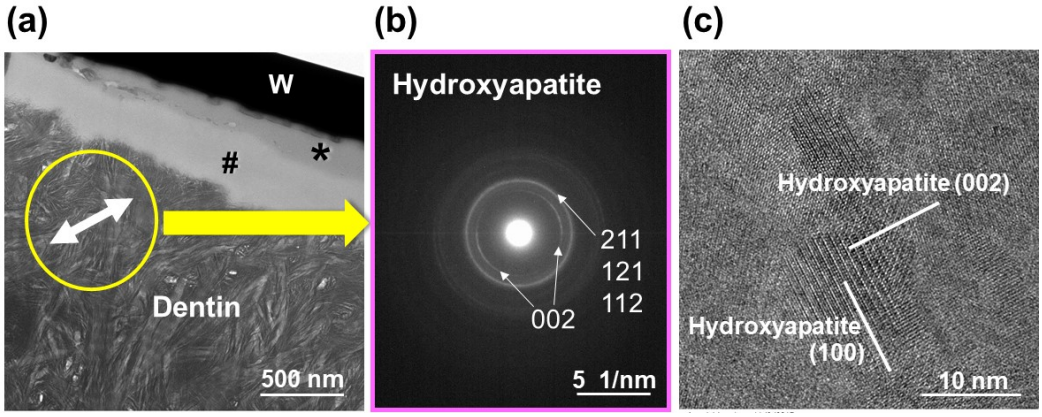

Figure 7 (a) Cross-sectional bright-field TEM image, (b) SAED pattern obtained from the circled area in (a), and (c) HRTEM image of the unprocessed dentin substrate. Two-way arrow in (a) indicates the direction of *c*-axis orientation of hydroxyapatite nanocrystals. W, *, and # in (a) indicate the W coating, the protective ink layer, and the organic layer, respectively.

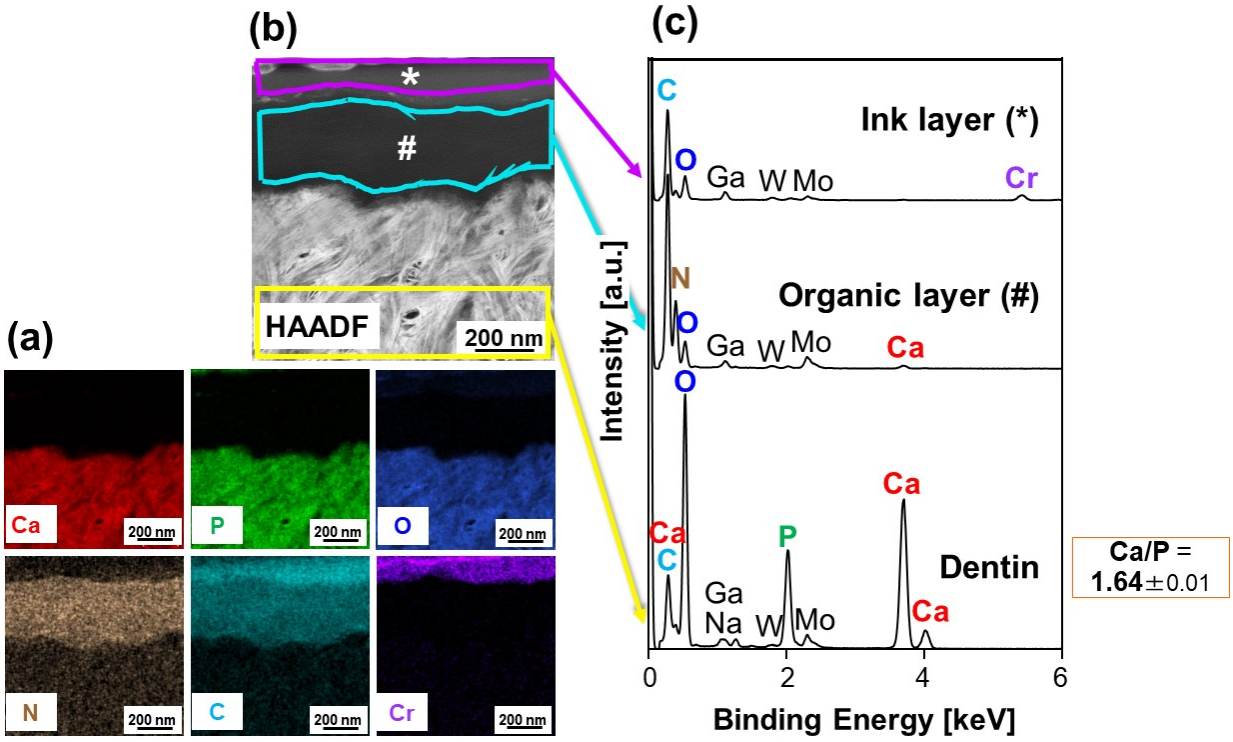

Figure 8 (a) Cross-sectional STEM-EDX elemental mappings (Ca, P, O, N, C, Cr), (b) the corresponding HAADF image, and (c) STEM-EDX spectra of the boxed areas in (b), of the unprocessed dentin substrate. * and # in (b) indicate the protective ink layer and the organic layer, respectively. The averaged Ca/P elemental ratio in the right-most box in (c) was calculated from the peak areas of Ca and P in the STEM-EDX spectra.

The unprocessed dentin substrate had a demineralized collagenous layer on its surface. As seen in Figures 7a and 8, two different layers composed of light elements existed on the dentin surface: a nitrogen (N)-containing organic layer (lower layer, marked with #) and a Cr-containing oil-based ink layer (upper layer, marked with *). In the cross-sectional STEM-EDX elemental mappings, the organic and ink layers were differentiated by the N and Cr elemental distributions (Figure 8a). As mentioned in Section 2.6, the ink was deposited on the substrates as a protective layer just before the FIB processing. Thus, the underlying N-containing organic layer existed on

the surface of the unprocessed (as-prepared) dentin substrate. This organic layer was composed mainly of C, N, and O, along with trace amounts of Ca and P (Figure 8c). These results indicate that the dentin substrate had a surface layer rich in organic components (N, C) and deficient in hydroxyapatite (Ca, P), as compared to the inner region. The N-containing organic layer is likely a demineralized collagenous layer formed as a consequence of hydroxyapatite dissolution from the dentin surface during the surface cleaning with EDTA. Demineralization of dentin in the EDTA solution is likely to occur because EDTA is a mild acid known to react with calcium ions of dentinal hydroxyapatite, forming soluble calcium chelates [33]; which is why EDTA has been used clinically as a smear removal agent.

3.5. Cross-sectional analyses of the LAB-processed dentin substrate

The LAB process induced the formation of a submicron-thick layer on the dentin surface. As seen in the cross-sectional bright-field TEM images (Figure 9), a continuous and uniform layer, slightly thinner than 1 μm, formed over the curved dentin surface after the LAB process. Based on the XRD results (Figure 3), this layer can be identified as hydroxyapatite. From the magnified image (lower right in Figure 9), the surface layer consisted of needle-like nanocrystals whose thickness, density, and orientation differed in its upper and lower regions. In the underlying dentin region of the LAB-processed substrate, no obvious structural changes were observed. In the lower magnification bright-field TEM images (Figure 9 top), micro-holes of dentinal canaliculi (indicated by arrows) were observed for both substrates, before and after the LAB process. The higher magnification images of both substrates (Figure 9 bottom) show needle-like structures typical of dentinal apatite and D-band structure (alternate dark and light bands with a period of approximately 67 nm [34,35]) typical of type I collagen fibrils (see dotted circles), which

corresponds to a previous report on dentin [36]. It is also worth noting that the dentin region of the LAB-processed substrate did not show an apparent destructive damage.

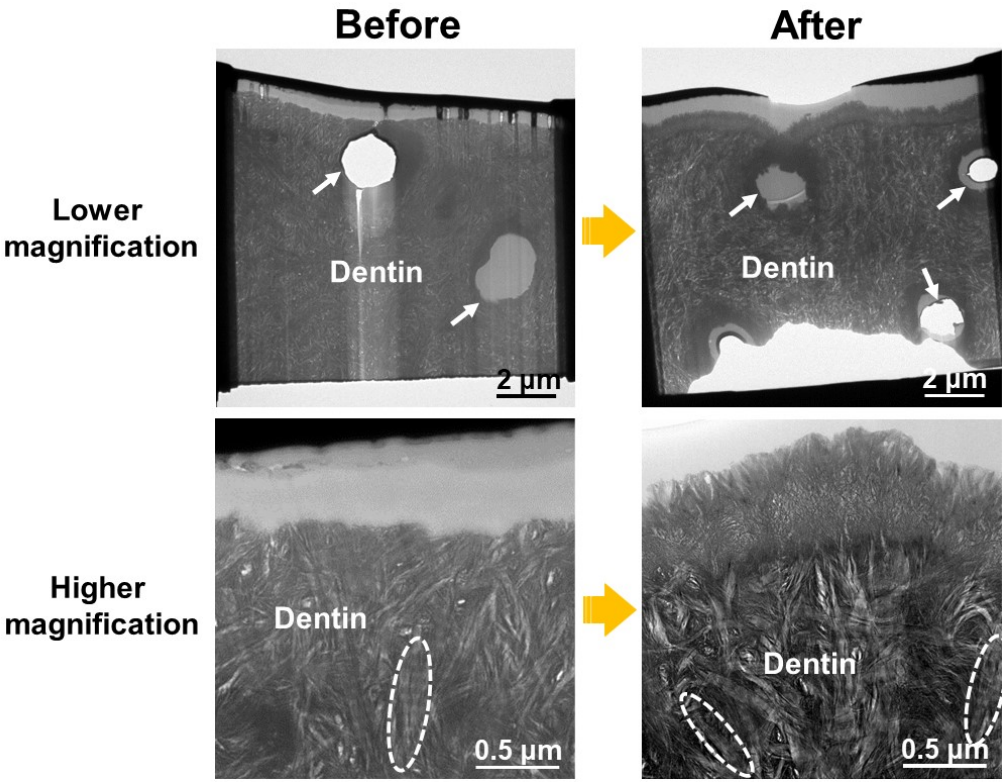

Figure 9 Higher and lower magnifications of cross-sectional bright-field TEM images of the dentin substrates before and after the LAB process. Arrows indicate dentinal tubules, and dotted circles indicate D-band structure typical of type I collagen fibrils.

The submicron-thick layer formed on the LAB-processed dentin substrate consisted of *c*-axis-oriented needle-like hydroxyapatite nanocrystals. As shown in the cross-sectional bright-field TEM image (Figure 10a), the upper region of the layer was filled with densely assembled needle-like nanocrystals perpendicular to the dentin surface. This region presented a lattice pattern corresponding to the (0 0 2) and (1 0 0) planes of hydroxyapatite in the HRTEM image (Figure

10c). The lower region of the layer, *i.e.*, an intermediate region between the layer's upper region and the dentin, consisted of finer nanocrystals that were sparser and more randomly oriented than those in the upper region. As confirmed by the SAED results (Figures 10a and 10b), nanocrystals in both the upper and lower regions of the layer were hydroxyapatite with weak *c*-axis orientation along the direction perpendicular to the substrate surface (two-way arrows). This agrees with the XRD results (Figure 3). According to the STEM-EDX results (Figures 11b and 11c), the Ca/P elemental ratio was calculated as 1.52 ± 0.02 and 1.56 ± 0.06 in the lower and upper regions of the layer, respectively, which were slightly lower than that of the underlying dentin region (1.62 ± 0.01).

The N-containing organic layer on the unprocessed dentin surface disappeared after the LAB process. As revealed by the Cr elemental distribution (Figure 11a), the uppermost layer (* in Figure 11b) was not the N-containing organic one but the Cr-containing ink coating. The hydroxyapatite layer was located directly underneath the ink as revealed by the Ca, P, and O distributions in Figure 11a. This hydroxyapatite layer was spontaneously integrated with the underlying dentin without any apparent boundaries. In the STEM-EDX mapping of N (Figure 11a), no layer rich in N was found at the interface between the hydroxyapatite layer and the underlying dentin. That is, the N-containing organic layer did not exist on the LAB-processed dentin surface, although it existed on the surface of the unprocessed dentin substrate (Figure 8). It is likely that the organic layer disappeared due to laser ablation in the LAB process.

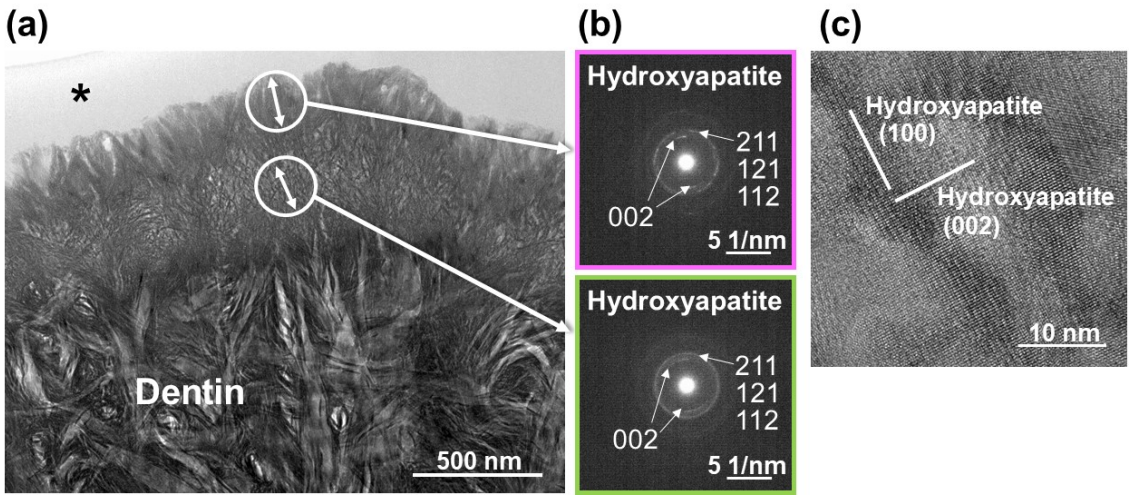

Figure 10 (a) Cross-sectional bright-field TEM image, (b) SAED patterns obtained from the circled areas in (a), and (c) HRTEM image (upper region of the surface layer), of the LAB-processed dentin substrate. Two-way arrows in (a) indicate the direction of *c*-axis orientation of hydroxyapatite nanocrystals, and * indicates the protective ink layer.

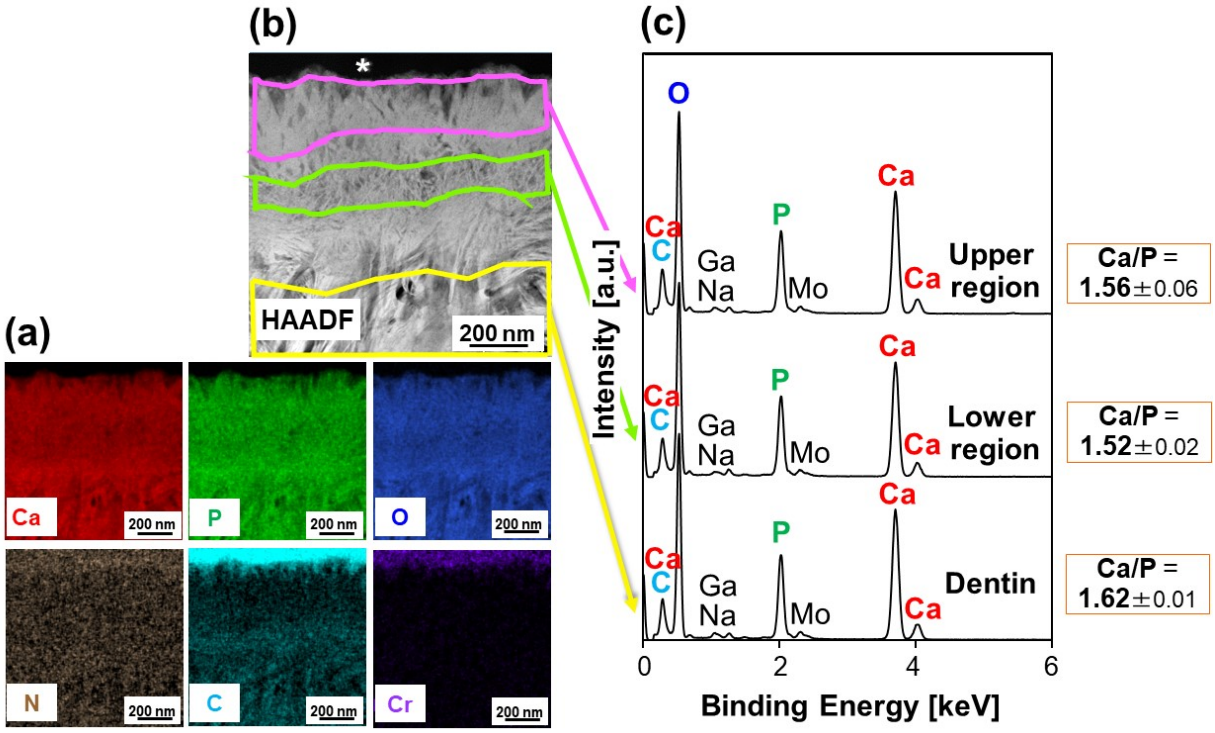

Figure 11 (a) Cross-sectional STEM-EDX elemental mappings (Ca, P, O, N, C, Cr), the corresponding HAADF image, and (c) STEM-EDX spectra of the boxed areas in (b), of the LAB-

processed dentin substrate. * in (b) indicates the protective ink layer. The averaged Ca/P elemental ratios in the right-most boxes in (c) were calculated from the peak areas of Ca and P in the STEM-EDX spectra.

3.6. Estimated mechanism of pseudo-biomineralization

As described above, the LAB process induced the pseudo-biomineralization on the human dentin surface within 30 min. The surface and cross-sectional analyses revealed that the mineralized layer formed on the dentin substrate consisted of hydroxyapatite needle-like nanocrystals with weak *c*-axis orientation. Below is the estimated mechanism of the laser-assisted biomineralization on the dentin surface.

The unprocessed (as-prepared) dentin substrate had an organic collagenous layer (Figures 7a and 8) that was a result of the demineralization during the EDTA surface-cleaning process. When this substrate was immersed in the CP solution and no laser irradiation was carried out, surface biomineralization did not occur within 30 min (Figure 5). This might be explained by the fact that the dentinal hydroxyapatite nanocrystals that can act as seed crystals were embedded under the collagenous layer on the substrate surface (Figure 8). Note that the CP solution is a metastable supersaturated solution that remains transparent, without homogeneous CaP nucleation, for weeks. In the LAB process, the collagenous layer was etched most likely due to laser ablation within 30 min (Figures 6 and 11). During the same period, biomineralization was induced on the substrate surface (Figures 2-3, 9-11). We consider that CaPs nucleated on the laser-activated collagenous layer and/or dentinal hydroxyapatite nanocrystals exposed to the liquid—solid interface. At this stage, laser irradiation should have an accelerating effect on CaP nucleation and crystal growth by heating the surface and the surrounding solution [14,19-21,24]. This is because

a rise in solution temperature increases not only the mass transfer rate but also the degree of supersaturation, as the solubility of hydroxyapatite is reduced when increasing the temperature [37,38]. Heat generation in the CP solution was experimentally confirmed; the solution temperature was elevated from 25 to 33ºC in the LAB process even with the use of the constant temperature water bath. According to the relatively small Ca/P elemental ratio (CaP = 1.52 ± 0.02) of the layer's lower region (intermediate region between the layer's upper region and the dentin), the initially formed mineral phase was calcium-deficient hydroxyapatite and may contain precursors, such as amorphous CaP and OCP, although they were not detected in this study. In the final layer, needle-like hydroxyapatite nanocrystals assembled (sparsely in the lower region and densely in the upper one) and were oriented with their *c*-axes perpendicular to the substrate surface (poorly in the lower region and highly in the upper one) as depicted in Figure 10. This is because of the effect of geometric selection of crystals [39].

In a preliminary study, we found that a sintered hydroxyapatite substrate formed plate-like OCP crystals, not hydroxyapatite, after the LAB process even under the same irradiation conditions to the ones used in this study [22]. In other words, the mineral phase formed by the LAB process was different for the dentin substrate and the sintered hydroxyapatite substrate in spite of their compositional similarity. We believe that the collagenous layer on the pristine dentin substrate played a certain role in the LAB process and affected the final mineral phase. Other factors possibly influencing the final mineral phase include the natural dentin color, and the presence of dentinal tubules, non-mineral components (collagen, water, etc.) and trace minerals (F, Mg, etc.), as they can affect the laser absorption and/or CaP nucleation and growth kinetics. Further studies are needed to shed light on the mechanism of laser-assisted pseudo-biomineralization on the dentin surface.

3.7. Advantages and potential of the LAB process

The LAB process may be used for tooth surface modification with biocompatible hydroxyapatite *via* laser-assisted pseudo-biomineralization. As described above, a submicron-thick hydroxyapatite layer was successfully formed on the dentin surface using this process. According to our previous results, a LAB-processed polymer substrate exhibits better cytocompatibility with osteoblastic cells *in vitro* than the unprocessed substrate, due to the surface hydroxyapatite layer [20]. A simulated body fluid test [5] suggested osteoconductivity of this surface-mineralized polymer substrate [20]. In addition, hydroxyapatite-coated polymers prepared using the CP solution as a reaction medium showed good biocompatibility with the soft tissue of rats *in vivo* [40-42]. Based on the above, and on previous numerous reports on hydroxyapatite [1-4], the LAB-processed dentin substrate likely exhibits good biocompatibility and osteoconductivity through the surface hydroxyapatite layer, although this should be assessed in future *in vitro* and *in vivo* studies.

The present LAB process has several advantages for tooth surface modification over conventional CaP coating techniques. This process is carried out under normal pressure and temperature using the CP solution: a physiological salt solution supplemented with biomineral ions and a buffering agent. With the stimulating effect of laser irradiation, biomineralization is rapidly induced on the dentin surface, leading to the formation of a submicron-thick hydroxyapatite layer in a one-step procedure within only 30 min. This represents a practical advantage over the conventional biomimetic processes that do not involve laser irradiation [6-9,40-42]. In addition, different from the majority of conventional CaP coating techniques [10,11], the LAB process induces area-specific biomineralization, that is, the mineralized region is confined to the laser-

irradiated area on a material surface [14,15,20]. Furthermore, the LAB process could be useful for the fabrication of mineralized surfaces with additional functionality *via* the immobilization of bioactive substances on the surface [22,23]. This could be easily done by adding the bioactive substances at an appropriate concentration to the CP solution. For instance, we prepared a fluoride-immobilized hydroxyapatite layer with antibacterial activity, because of the fluoride, *via* the LAB process using a CP solution supplemented with fluoride ions [22]. As CaP coating techniques for tooth surfaces, some other processes have been proposed, *e.g.*, CaP particle-based processes [43,44], a CaP paste-based process [45], a CaP sheet-based process [46], and CaP solution-based processes [47,48]. However, it is difficult to find a clinically applicable process that meet all the requirements for tooth surface modification: area-specificity of the coating, process simplicity, and safety of the source reagents. Considering the advantages described above, the LAB process may be a useful new tool for tooth surface modification and functionalization *via in situ* pseudo-biomimeralization, although further studies are required.

4. Conclusion

The unprocessed (as-prepared) dentin substrate had a demineralized collagenous layer on its surface that was exposed because of surface cleaning with EDTA. During the LAB process, the collagenous layer was removed most likely due to laser ablation and replaced with a submicron-thick hydroxyapatite layer through the pseudo-biomineralization at the dentin–liquid interface. The thus-formed mineralized layer on the dentin surface consisted of needle-like hydroxyapatite nanocrystals whose *c*-axes were weakly oriented normal to the surface. Also, the layer spontaneously integrated with the underlying dentin. The LAB process induces rapid pseudo-

biomimeralization on the dentin surface; hence, it may be a useful new tool for tooth surface modification and functionalization.

Disclosure The authors report no conflicts of interest in this work.

Acknowledgments This work was supported by JSPS KAKENHI (JP15F15331, JP17H02093, 19K22991) and The Amada Foundation, Japan.

References

1. H. Aoki, Science and Medical Applications of Hydroxyapatite, Ishiyaku Euroamerica, 1992.

2. S.V. Dorozhkin, Calcium orthophosphates in dentistry, J. Mater. Sci. Mater. Med., 24 (2013) 1335–1363.

3. S.M. Best, A.E. Porter, E.S. Thian, J. Huang, Bioceramics: Past, present and for the future, J. Eur. Ceram. Soc., 28 (2008) 1319–1327.

4. W. Habraken, P. Habibovic, M. Epple, M. Bohner, Calcium phosphates in biomedical applications: materials for the future?, Mater. Today, 19 (2016) 69–87.

5. T. Kokubo, H. Takadama, How useful is SBF in predicting in vivo bone bioactivity?, Biomater., 27 (2006) 2907–2915.

6. M. Tanahashi, T. Yao, T. Kokubo, M. Minoda, T. Miyamoto, T. Nakamura, T. Yamamuro, Apatite coating on organic polymers by a biomimetic process, J. Am. Ceram. Soc., 77 (1994) 2805–2808.

7. X.P. Wang, A. Ito, X. Li, Y. Sogo, A. Oyane, Signal molecules–calcium phosphate coprecipitation and its biomedical application as functional coating, Biofabrication, 3 (2011) 022001.

8. A. Oyane, X. Wang, Y. Sogo, A. Ito, H. Tsurushima, Calcium phosphate composite layers for surface-mediated gene transfer, Acta Biomater. 8 (2012) 2034–2046.

9. N. Koju, P. Sikder, Y. Ren, H. Zhou, S.B. Bhaduri, Biomimetic coating technology for orthopedic implants, Curr. Opin. Chem. Eng., 15 (2017) 49–55.

10. Sameer R. Paital, Narendra B. Dahotre, Calcium phosphate coatings for bio-implant applications: Materials, performance factors, and methodologies, Mater. Sci. Eng. R, 66 (2009) 1–70.

11. S.V. Dorozhkin, Calcium orthophosphate deposits: Preparation, properties and biomedical applications, Mater. Sci. Eng. C, 55 (2015) 272–326.

12. H.M. Kim, K. Kishimoto, F. Miyaji, T. Kokubo, T. Yao, Y. Suetsugu, J. Tanaka, T. Nakamura, Composition and structure of apatite formed on organic polymer in simulated body fluid with a high content of carbonate ion, J. Mater. Sci. Mater. Med., 11 (2000) 421–426.

13. A. Oyane, Y. Ishikawa, A. Yamazaki, Y. Sogo, K. Furukawa, T. Ushida, A. Ito, Reduction of surface roughness of a laminin–apatite composite coating via inhibitory effect of magnesium ions on apatite crystal growth, 4 (2008) 1342-1348.

14. A. Oyane, I. Sakamaki, Y. Shimizu, K. Kawaguchi, N. Koshizaki, Liquid-phase laser process for simple and area-specific calcium phosphate coating. J. Biomed. Mater. Res. A, 2012, 100A, 2573–2580.

15. M. Nakamura, A. Oyane, Physicochemical fabrication of calcium phosphate-based thin layers and nanospheres using laser processing in solutions, J. Mater. Chem. B, 4 (2016) 6289–6301.

16. M. Uchida, A. Oyane, H.M. Kim, T. Kokubo, A. Ito, Biomimetic coating of laminin–apatite composite on titanium metal with excellent cell adhesive property, Adv. Mater., 16 (2004) 1071–1074.

17. E. Pecheva, T. Petrov, C. Lungu, P. Montgomery, L. Pramatarova, Stimulated in vitro bone-like apatite formation by a novel laser processing technique, Chem. Eng. J., 137 (2008) 144–153.

18. B.H. Lee, A. Oyane, H. Tsurushima, Y. Shimizu, T. Sasaki, N. Koshizaki, A new approach for hydroxyapatite coating on polymeric materials using laser-induced precursor formation and subsequent aging, ACS Appl. Mater. Interfaces, 1 (2009) 1520–1524.

19. A. Oyane, I. Sakamaki, A. Pyatenko, M. Nakamura, Y. Ishilawa, K. Kawaguchi, N. Koshizaki, Laser-assisted calcium phosphate deposition on polymer substrates in supersaturated solutions, RSC Adv., 4 (2014) 53645–53648.

20. A. Oyane, M. Nakamura, I. Sakamaki, Y. Shimizu, S. Miyata, H. Miyaji, Laser-assisted wet coating of calcium phosphate for surface-functionalization of PEEK, Plos One, 13 (2018) e0206524.

21. A. Oyane, I. Sakamaki, Y. Shimizu, K. Kawaguchi, Y. Sogo, A. Ito, N. Koshizaki, Laser-assisted biomimetic process for calcium phosphate coating on a hydroxyapatite ceramic, Key Eng. Mater., 529–530 (2013) 217–222.

22. A.J. Nathanael, A. Oyane, M. Nakamura, K. Shitomi, H. Miyaji, Rapid and area-specific coating of fluoride-incorporated apatite layers by a laser-assisted biomimetic process for tooth surface functionalization, Acta Biomaterialia, 79 (2018) 148–157.

23. A. Oyane, N. Matsuoka, K. Koga, Y. Shimizu, M. Nakamura, K. Kawaguchi, N. Koshizaki, Y. Sogo, A. Ito, H. Unuma, Laser-assisted biomimetic process for surface functionalization of titanium metal, Coll. Interf. Sci. Comm., 4 (2015) 5–9.

24. M. Mahanti, M. Nakamura, A. Pyatenko, I. Sakamaki, K. Koga, A. Oyane, The mechanism underlying calcium phosphate precipitation on titanium via ultraviolet, visible, and near infrared laser-assisted biomimetic process, J. Phys. D: Appl. Phys., 49 (2016) 304003.

25. A.J. Nathanael, A. Oyane, M. Nakamura, K. Koga, E. Nishida, S. Tanaka, H. Miyaji, Calcium phosphate coating on dental composite resins by a laser-assisted biomimetic process, Helyon, 4 (2018) e00734.

26. B.L. Pihlstrom, B.S Michalowicz, N.W. Johnson, Periodontal diseases, Lancet, 366 (2005) 1809–1820.

27. S.S. Steiner, M. Crigger, J. Egelberg, Connective tissue regeneration to periodontally diseased teeth, J. Periodont. Res., 16 (1981) 109–116.

28. J. Caton, S. Nyman, Histometric evaluation of periodontal surgery Ⅰ. The modified Widman flap procedure, J. Clin. Periodontol., 7 (1980) 224–231.

29. T. Fujita, S. Yamamoto, M. Ota, Y. Shibukawa, S. Yamada, Coverage of gingival recession defects using guided tissue regeneration with and without adjunctive enamel matrix derivative in a dog model, Int. J. Periodont. Restorative Dent., 31 (2011) 247–253.

30. Th. Leventouri, A. Antonakos, A. Kyriacou, R. Venturelli, E. Liarokapis, V. Perdikatsis, Crystal structure studies of human dental apatite as a function of age, Inter. J. Biomaterials, 2009 (2009) 698547.

31. M.C. Chang, J. Tanaka, FT-IR study for hydroxyapatite/collagen nanocomposite cross-linked by glutaraldehyde, Biomaterials, 23 (2002) 4811–4818.

32. L. Bachmann, R. Diebolder, R. Hibst, D.M. Zezell, Infrared absorption bands of enamel and dentin tissues from human and bovine teeth, Appl. Spectroscopy Rev., 38 (2003) 1–14.

33. Z. Mohammadi, S. Shalavi, H. Jafarzadeh, Ethylenediaminetetraacetic acid in endodontics, Eur. J. Dent., 7 (Suppl 1) (2013) S135–S142.

34. T. Ushiki, Collagen fibers, reticular fibers and elastic fibers. A comprehensive understanding from a morphological viewpoint, Arch. Histol. Cytol., 65 (2002) 109–126.

35. D.F. Holmes, C.J. Gilpin, C. Baldock, U. Ziese, A.J. Koster, K.E. Kadler, Corneal collagen fibril structure in three dimensions: Structural insights into fibril assembly, mechanical properties, and tissue organization, 98 (2001) 7307–7312.

36. R.K. Nalla, A.E. Porter, C. Daraio, A.M. Minor, V. Radmilovic, E.A. Stach, A.P. Tomsia, R.O. Ritchie, Ultrastructural examination of dentin using focused ion-beam cross-sectioning and transmission electron microscopy, Micron, 36 (2005) 672–680.

37. H. McDowell, T. Gregory, W. Brown, Solubility of $Ca_5(PO_4)_3OH$ in the system $Ca(OH)_2$–H_3PO_4–H_2O at 5, 15, 25 and 37°C, J. Res. Nat. Bureau Stand., 81 (1972) 273–281.

38. M.J.J.M. Van Kemenade, P.L. De Bruyn, A kinetic study of precipitation from supersaturated calcium phosphate solutions, J. Col. Interf. Sci., 118 (1987) 564–585.

39. C.V. Thompson, Structure evolution during processing of polycrystalline films, Annu. Rev. Mater. Sci., 30 (2000) 159–190.

40. K. Sasaki, A. Oyane, K. Hyodo, A. Ito, Y. Sogo, M. Kamitakahara1, K. Ioku, Preparation and biological evaluation of a fibroblast growth factor-2–apatite composite layer on polymeric material, Biomed. Mater., 5 (2010) 065008.

41. A. Oyane, K. Hyodo, M. Uchida, Y. Sogo, A. Ito, Preliminary *in vivo* study of apatite and laminin-apatite composite layers on polymeric percutaneous implants, J. Biomed. Mater. Res. Appl. Biomater., 97B (2011) 96–104.

42. A.J. Nathanael, A. Oyane, M. Nakamura, I. Sakamaki, E. Nishida, Y. Kanemoto, H. Miyaji, In vitro and in vivo analysis of mineralized collagen-based sponges prepared by a plasma- and precursor-assisted biomimetic process, ACS Appl. Mater. Interf., 9 (2017) 22185−22194.

43. R. Akatsuka, H. Ishihata, M. Noji, K. Matsumura, T. Kuriyagawa, K. Sasaki, Effect of hydroxyapatite film formed by powder jet deposition on dentin permeability, Eur. J. Oral Sci., 120 (2012) 558–562.

44. L. Li, C. Mao, J. Wang, X. Xu, H. Pan, Y. Deng, X. Gu, R. Tang, Bio-inspired enamel repair via Glu-directed assembly of apatite nanoparticles: an approach to biomaterials with optimal characteristics, Adv. Mater., 23 (2011) 4695–4701.

45. K. Yamagishi, K. Onuma, T. Suzuki, F. Okada, J. Tagami, M. Otsuki, P. Senawangse, A synthetic enamel for rapid tooth repair, Nature, 433 (2005) 819.

46. S. Hontsu, K. Yoshikawa, N. Kato, Y. Kawakami, T. Hayami, H. Nishikawa, M. Kusunoki, K. Yamamoto, Restoration and conservation of dental enamel using a flexible apatite sheet, J. Aust. Ceram. Soc., 47 (2011) 11–13.

47. Y. Fan, Z. Sun, J. Moradian-Oldak, Controlled remineralization of enamel in the presence of amelogenin and fluoride, Biomaterials, 30 (2009) 478–483.

48. M. Sun, N. Wu, H. Chen, Laser-assisted rapid mineralization of human tooth enamel, Sci. Rep., 7 (2017) 9611.